J Neuropathol Exp Neurol

Vol. 70, No. 5
May 2011
pp. 349–359

ORIGINAL ARTICLE

Autophagy in Spinal Cord Motor Neurons in Sporadic Amyotrophic Lateral Sclerosis

Shoichi Sasaki, MD, PhD

Abstract

To assess the potential role of autophagy in amyotrophic lateral sclerosis (ALS), lumbar spinal cords in a total of 19 sporadic ALS cases and 27 age-matched controls were investigated. Immunohistochemical analysis using antibodies to the markers of autophagy microtubule-associated protein light chain 3 (LC3) and p62 was performed on samples from 12 ALS and 15 controls. Electron microscopy was performed on samples from 16 ALS and 15 controls, including overlapping cases. In the ALS cases, the somata of normal-appearing and degenerated motor neurons and round bodies were occasionally immunostained for LC3; round bodies and skein-like inclusions were immunostained for p62. By electron microscopy, all 16 ALS patients showed features of autophagy in the cytoplasm of normal-appearing motor neurons and, more frequently, in degenerated motor neurons. Autophagosomes surrounded by a double-membrane and autolysosomes isolated by a single membrane contained sequestered cytoplasmic organelles, such as mitochondria and ribosome-like structures. These autophagy features were also found in close association with the characteristic inclusions of ALS (i.e. round bodies, skein-like inclusions, and Bunina bodies); honeycomb-like structures also occasionally showed autophagy-associated features. Normal-appearing anterior horn neurons in control patients showed no autophagy features. Thus, autophagy seems to be activated and upregulated in the cytoplasm of motor neurons and may be involved in the mechanisms of neurodegeneration of motor neurons in sporadic ALS.

Key Words: Amyotrophic lateral sclerosis, Autolysosome, Autophagosome, Autophagy, Electron microscopy, LC3, p62.

INTRODUCTION

There are 2 main pathways for the degradation of intracellular components in eukaryotic cells: the ubiquitin-proteasome and autophagy-lysosome pathways. The ubiquitin-proteasome system, which accounts for most of the selective intracellular protein degradation, plays crucial roles in the degradation of short-lived regulatory proteins and abnormal proteins that need to be eliminated from the cells (1). By contrast, although the degradation of cytoplasmic proteins and organelles is achieved through several pathways such as macroautophagy, microautophagy and chaperone-mediated autophagy (2), the intracellular bulk degradation of cytoplasmic constituents is mediated largely by macroautophagy, generally referred to as autophagy. Macroautophagy delivers cytoplasmic components to the lysosome for degradation in eukaryotic cells and is believed to be the main pathway among several subtypes of autophagy.

Autophagy consists of several sequential steps. The initial step is the elongation of the isolation membrane, called phagophore, which enwraps small portions of cytoplasmic organelles. Its edges then fuse into the formation of double-membrane structures called autophagosomes. Finally, the outer membrane of the autophagosome fuses with lysosomes to form autolysosomes and the sequestered cytoplasmic materials are degraded by the lysosomal hydrolases, together with the inner membrane of the autophagosome; this is followed by the generation of amino acids that are recycled for macromolecular synthesis and energy production (3, 4). In contrast to the ubiquitin-proteasome system, because autophagosomes engulf portions of cytoplasmic organelles, autophagy is generally thought to be a nonselective or less selective degradation system.

Autophagy is upregulated in response to cellular stress and can provide an adaptive strategy for cell survival; however, it may also directly or indirectly contribute to cell death (4–6). With its dual roles in life and death, autophagy plays central roles in various physiological processes such as development and aging, and in many pathologic conditions and processes including cancer, infectious diseases, and excitotoxicity (7–12). Recent genetic studies in mice have documented the importance of constitutive or basal autophagy in neurons, in which the loss of autophagy results in severe neurodegeneration (13, 14). On the other hand, autophagy is upregulated in neurons in several conditions, including nutrient starvation, development, and neurodegeneration (15, 16).

Very little is known about autophagy in amyotrophic lateral sclerosis (ALS) (17–20). This study investigated the lumbar spinal cord in patients with sporadic ALS and age-matched control patients using immunohistochemistry with antibodies to microtubule-associated protein light chain 3 (LC3), a marker for autophagosome (21, 22), and p62, which directly interacts with LC3 and is degraded by autophagy-lysosome pathway (23). Electron microscopy (EM) was also used to characterize the morphology of autophagy in ALS cases. This is the first report on autophagic processes commonly observed in the cytoplasm of motor neurons in patients with sporadic ALS.

From the Department of Neurology, Tokyo Women's Medical University, Tokyo, Japan.
Send correspondence and reprint requests to: Shoichi Sasaki, MD, PhD, Department of Neurology, Tokyo Women's Medical University, 8-1 Kawada-cho, Shinjuku-ku, Tokyo 162-8666, Japan; E-mail: ssasaki@nij.twmu.ac.jp
This work was supported by a Grant-in-Aid for General Scientific Research from The Ministry of Education, Culture, Sports, Science, and Technology.

MATERIALS AND METHODS

Light Microscopy

The lumbar levels (L1–L5) of the spinal cord of 19 autopsied patients with sporadic ALS (aged 49–83 years; mean, 68.1 ± 8.0 years) and 27 age-matched control patients (aged 48–83 years; mean, 65.2 ± 10.8 years) were investigated. The spinal cords were fixed in formalin at autopsy. After fixation, the lumbar spinal cords were embedded in paraffin. Five-micrometer-thick sections were stained with hematoxylin and eosin (H&E) and Klüver-Barrera.

Immunohistochemistry

Paraffin-embedded spinal cord sections of 15 controls (aged 48–83 years; mean, 70.2 ± 9.6 years) and 12 ALS patients (aged 49–83 years; mean, 66.8 ± 9.0 years) were immunostained (Table 1). The antibodies used were a rabbit polyclonal anti-LC3 antibody (1:20000; Medical Biological Laboratories, Nagoya, Japan) (to avoid nonspecific staining, the concentration was much lower than that recommended by the manufacturer), and a guinea pig polyclonal anti–N-terminal domain of human p62 antibody (1:3000, GP62-N; Progen Biotechnik, Heidelberg, Germany). The sections were deparaffinized, rehydrated, quenched for 10 minutes at 4°C in 3% H_2O_2, rinsed in phosphate-buffered saline, pH 7.6, pretreated for 20 minutes at room temperature with 5% skim milk in phosphate-buffered saline, and then incubated overnight at 4°C with the primary antibodies. For enhancement, microwave treatment (500 W, 95°C, 20 minutes) in 10 mmol/L of citrate buffer (pH 6.0) was performed. Staining with the anti-LC3 antibody was visualized by the polymer immunocomplex method using the ENVISION system (DAKO, Glostrup, Denmark) as follows: the first incubation with primary antibody for 2 hours at room temperature was followed by washing in Tris-buffered saline and incubation with secondary antibody. For anti-p62, sections were incubated with biotinylated secondary antibody and then subjected to the avidin-biotinylated horseradish peroxidase complex method (Vector Laboratories, Burlingame, CA). The final chromogen was 3,3′-diaminobenzidine tetrahydrochloride. Sections from which the primary antibody was omitted served as negative reaction controls. All sections were counterstained with hematoxylin.

TABLE 1. Clinical and Pathologic Data on Cases Studied Using Immunohistochemistry

Controls	Age, yr	Sex	Postmortem Delay	Diagnosis
1	60	M	1 h 57 min	Hepatic cancer
2	70	F	10 h 40 min	Pancreatic cancer
3	83	M	7 h 42 min	Burns
4	76	M	6 h 20 min	Rupture of thoracic aneurysm
5	69	M	14 h 30 min	Stomach cancer
6	58	F	9 h 48 min	Ovarian cancer
7	64	M	9 h 10 min	Hepatic cancer
8	48	F	4 h	Congestive heart failure
9	71	F	1 h 35 min	Rupture of abdominal aneurysm
10	80	M	1 h 30 min	Esophageal cancer
11	75	M	2 h 10 min	Rupture of abdominal aneurysm
12	81	M	2 h 30 min	Large intestine cancer
13	73	M	13 h	Sepsis (MRSA)
14	78	M	1 h 46 min	Rupture of abdominal aneurysm
15	67	M	2 h 35 min	Bacterial septic shock
Mean ± SD	70.2 ± 9.6			
ALS	**Age, yr**	**Sex**	**Clinical Course, mo**	**Pathologic Findings**
1	83	M	10	B, L
2	49	M	16	B, L
3	61	M	21	B, L, S
4	71	F	26	B, L
5	72	M	28	B, L, S
6	65	M	29	L
7	62	M	30	B, L
8	68	M	33	B, L
9	63	F	42	B, L
10	60	F	48	B
11	78	F	68	B, L
12	70	F	72	B, L, S
Mean ± SD	67.8 ± 8.0			

ALS, amyotrophic lateral sclerosis; B, Bunina body; F, female; L, Lewy body-like hyaline inclusion (round body); M, male; MRSA, methicillin-resistant *Staphylococcus aureus*; S, skein-like inclusion.

Electron Microscopy

The lumbar spinal cord was studied by EM in 16 patients with sporadic ALS (aged 49–83 years; mean, 68.7 ± 8.5 years), including 9 patients (Cases 3, 4, 6, 8, 9, 10, 13, 14, and 16) used in the immunohistochemical study, and 15 age-matched control patients (aged 44–80 years; mean, 62.7 ± 11.2 years); these included 3 controls (Cases 5, 11, and 12) used in the immunohistochemical study who died without having any known neurologic disease (Table 2). In all ALS and control cases, an autopsy was performed within 6 hours of death to minimize postmortem artifacts. The lumbar spinal cord (L1–L5) was fixed in 2% glutaraldehyde with phosphate buffer (pH 7.40) at the time of autopsy. After fixation, the anterior horns at each level of the lumbar spinal cord were sectioned transversely, postfixed in 1% osmium tetroxide for several hours, dehydrated, and embedded in epoxy resin. Each block was cut into serial semithin sections (approximately 1 μm thick). These sections were stained with toluidine blue. Appropriate portions of the sections were cut into ultrathin sections, which were then stained with uranyl acetate and lead citrate for EM. In the controls, a total of 173 normal-looking large anterior horn neurons and a total of 72 degenerated motor neurons showing chromatolytic change were studied. Electron microscopic photographs covering the whole area of the cytoplasm in each motor neuron were obtained under an original magnification of 5,000. Then the films were developed, and the pictures were enlarged to black and white photographic paper (13 × 18 cm) under final magnification of 9,500.

RESULTS

Light Microscopy

Bunina bodies, Lewy body-like inclusions (round bodies), and skein-like inclusions were observed in H&E-stained

TABLE 2. Clinical and Pathologic Data on Cases Studied by Electron Microscopy

Controls	Age, yr	Sex	Diagnosis	Pathology
1	60	M	Lung cancer	
2	54	F	Esophageal cancer	
3	53	M	Esophageal cancer	Autophagy
4	62	M	Lung cancer	
5*	78	M	Rupture of abdominal aneurysm	
6	80	M	Rupture of abdominal aneurysm	
7	68	F	Rupture of abdominal aneurysm	
8	62	M	Acute myocardial infarction	
9	54	F	Diabetes mellitus, sepsis	Autophagy
10	44	F	Ovarian cancer	
11*	75	M	Rupture of abdominal aneurysm	
12*	80	M	Esophageal cancer	
13	52	M	Constrictive cardiomyopathy	
14	57	M	Hepatic cancer	
15	62	F	Acute myocardial infarction	
Mean ± SD	67.2 ± 11.2			
ALS Cases	**Age, yr**	**Sex**	**Clinical Course, mo**	**Inclusions†**
1	70	F	6	◯B, ◯L, S
2	75	M	6	◯B, ◯L, S
3*	83	M	10	B, L, S
4*	49	M	16	B, L, S
5	69	M	17	◯B, S
6*	61	M	21	B, L, S
7	67	F	24	◯B, S
8*	71	F	26	B, S
9*	72	M	28	B, L, S
10*	62	M	30	B, S
11	76	F	30	◯B, S
12	76	F	32	◯B, S
13*	68	M	33	B, L, S
14*	63	F	42	B, L, S
15	59	F	65	◯B, ◯L
16*	78	F	68	B, L, S

*Cases also used in the immunohistochemical study.
†B, Bunina body; L, Lewy body-like (round) inclusion; S, skein-like inclusion. Circles indicate inclusions observed by both light and electron microscopes.
ALS, amyotrophic lateral sclerosis; F, female; M, male.

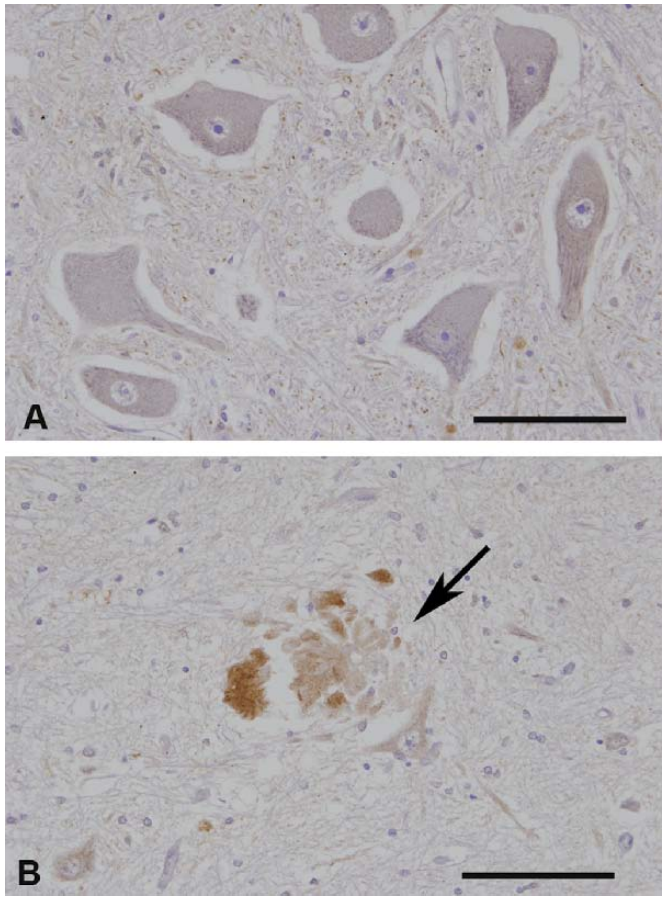

FIGURE 1. Control patients. **(A)** Normal-appearing large motor neurons are not immunostained for LC3. **(B)** A pericapillary rosette in the neuropil of the anterior horn is immunostained for LC3 (arrow). Bars = 100 μm.

sections in the cytoplasm of motor neurons in 18, 14, and 3 of 19 ALS patients, respectively (Tables 1 and 2). Skein-like inclusions were hardly recognized by H&E, whereas eosinophilic Bunina bodies and round bodies were easily detected. None of the control patients showed any inclusion body.

Immunohistochemistry

Except for 1 degenerated motor neuron in a single control case showing diffuse immunopositivity in the soma, neither small nor large motor neurons showed LC3 immunoreactivity in the cytoplasm of controls (Fig. 1A). On the other hand, pericapillary rosettes in the neuropil of anterior horns (24) were LC3-positive (Fig. 1B). In all control cases, anterior horn neurons were not immunostained for p62.

In the ALS cases, normal-appearing (Fig. 2) and degenerated anterior horn neurons were occasionally immunostained for LC3. Ectopic neurons in the white matter of the anterior column and abnormal structures such as colloid inclusions were also occasionally immunostained for LC3 (not shown). Pericapillary rosettes in anterior horns were also immunostained for LC3. Lewy body-like inclusions (round bodies) were almost always LC3-negative (Figs. 3A, B), with some exceptions (Figs. 3C, D). Bunina bodies and skein-like inclusions were not immunostained for LC3. On the other hand, round bodies (Figs. 4A, B) and skein-like inclusions (Figs. 4C, D) were p62-positive. Bunina bodies were p62-negative. Sections from which the primary antibodies (LC3 and p62) had been omitted showed no immunoreactivity.

Electron Microscopy

A total of 173 normal-looking large anterior horn neurons analyzed in control patient samples showed abundant Nissl bodies, mitochondria, lipofuscin granules, and lysosomes in the somata and exhibited no autophagic processes in the cytoplasm (Figs. 5A, B). In addition, a total of 72 degenerated motor neurons, probably affected by each disease process and/or medication such as anticancer drugs, showed chromatolytic change with an eccentric position of the nucleus, the fragmentation and the paucity of the rough endoplasmic reticulum (rER), abundant mitochondria, and neurofilaments in the cytoplasm; these neurons exhibited no autophagy-like structures (Figs. 6A, B). However, a motor neuron with large vacuolation in a single case and a degenerated motor neuron with electron-dense material resembling a Bunina body in another case showed autophagosome-like (Fig. 7A) and autolysosome-like (Fig. 7B) structures, respectively. No autophagy was observed in the myelinated axons of the anterior horn, anterior column, lateral column, or anterior roots of the control samples.

In ALS patients, as in the controls, normal-appearing large motor neurons contained abundant rER, mitochondria, lipofuscin granules, and lysosomes; degenerative motor neurons with central chromatolytic changes showed fragmentation and the paucity of rER, abundant mitochondria, and occasionally increased cytoplasmic neurofilaments. Both normal-appearing and degenerated motor neurons of all ALS patients exhibited inclusion bodies characteristic of ALS. Round bodies that consist of randomly arranged filaments associated with fine granules were observed in 10 of the 16 patients. Skein-like inclusions that consist of a bundle of densely packed filamentous structures running parallel to the longitudinal axis and tubular profiles on the transverse

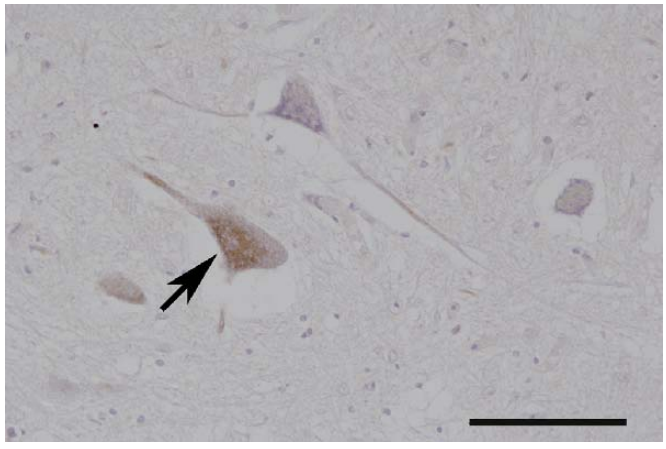

FIGURE 2. The cytoplasm of a normal-appearing large anterior horn neuron is immunostained for LC3 (arrow) in a patient with amyotrophic lateral sclerosis. Bar = 100 μm.

sections were found in 15 of the 16 ALS patients. All patients exhibited Bunina bodies that consist mainly of electron-dense granular or amorphous material usually surrounded or invaginated by vesicles and tubular structures.

Autophagosomes surrounded by a double membrane (Fig. 8) and autolysosomes surrounded by a single membrane (Fig. 9) were variably observed in the cytoplasm of all patients. In particular, the patients with a short clinical course and relatively well-preserved anterior horn neurons (Patients 1, 2, and 3) showed more numerous autophagosomes and autolysosomes. These autophagy-related structures were demonstrated under 4 circumstances. First, they were occasionally observed in the somata of normal-appearing large motor neurons (Figs. 8 and 9). They were usually scattered in the cytoplasm. Sequestered cytoplasmic organelles consisted of various kinds of structures such as mitochondria, ribosome-like structures (Fig. 8), and amorphous, vesicular, membranous, or multilamellar materials (Fig. 9). The space between the double membranes was usually translucent but occasionally contained amorphous or vesicular material. Second, they were more frequently observed in the cytoplasm of degenerated motor neurons with central chromatolytic change or pigmentary atrophy (Figs. 10A, B) than in normal-appearing motor neurons; they frequently clustered in the cytoplasm. Third, they were closely associated with ALS-characteristic inclusion bodies, that is, round bodies, skein-like inclusions, and Bunina bodies. Of 65 round bodies, 55 (approximately 85%) contained autophagosomes and/or autolysosomes inside (Fig. 11) and/or on the periphery. Skein-like inclusions were frequently engulfed by autophagosomes with a double-membrane (Figs. 12A, B) or autolysosomes with a single membrane (Fig. 12C). Of 72 Bunina bodies, 39 (approximately 54%) contained autophagy-related structures inside (Fig. 13) and/or on the periphery. Fourth, these structures were also observed within honeycomb-like structures (Fig. 14). No autophagy was observed in the normal-appearing myelinated axons of the anterior horn, anterior column, lateral column, and anterior root, but 1 of 6 round bodies observed in the swollen or normal-sized axons showed autophagosomes inside. Some swollen axons consisting of the accumulation of neurofilaments only occasionally contained autophagy-associated structures.

DISCUSSION

Recent studies indicate that in mammalian cells, autophagy serves 2 physiological purposes. The first, known

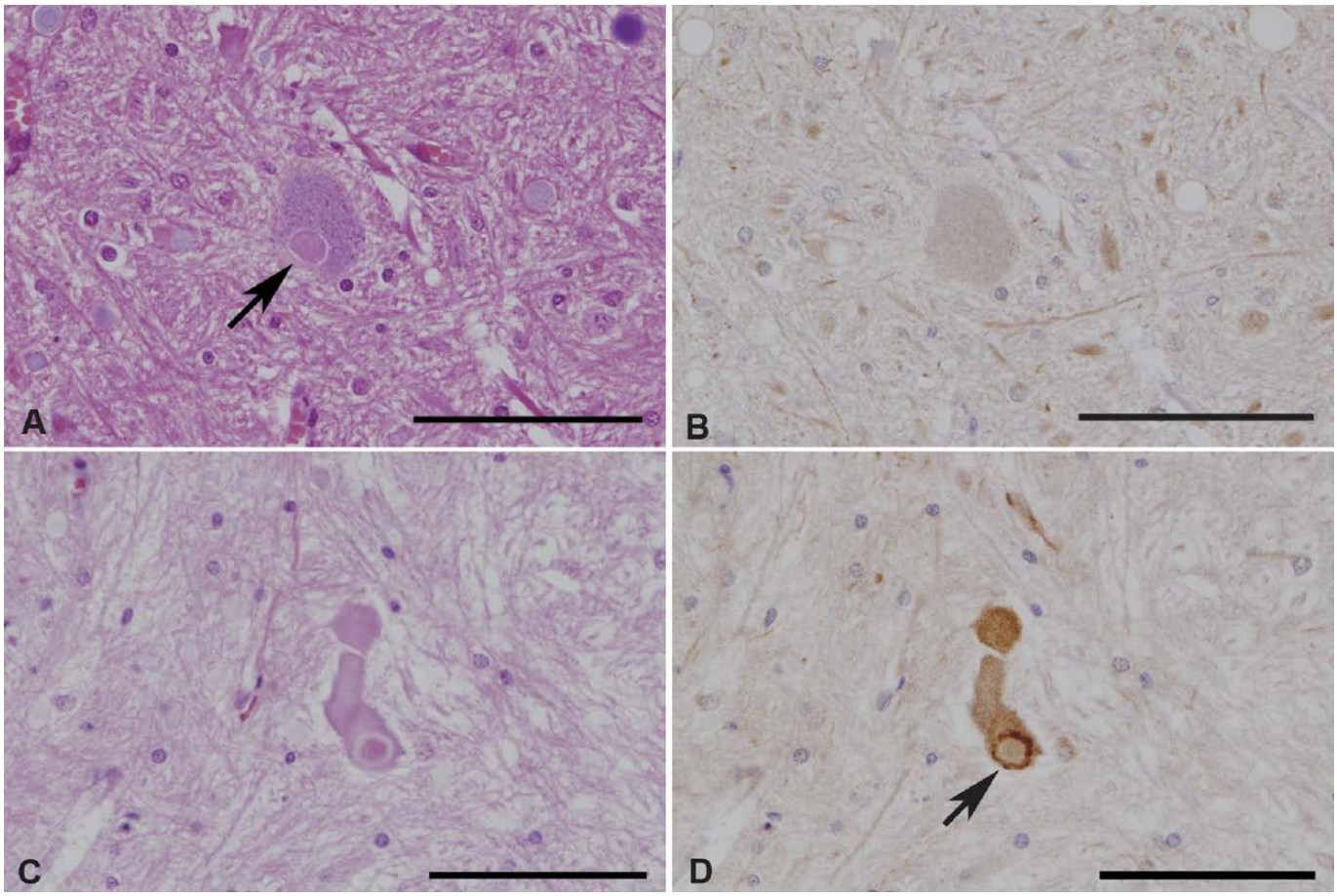

FIGURE 3. Amyotrophic lateral sclerosis patients. **(A, B)** A Lewy body-like hyaline inclusion (round body) (arrow) (**A**, H&E) is not immunostained for LC3 **(B)**. **(C, D)** The circumferential periphery of the round body in a swollen axon (**C**, H&E) is immunostained for LC3 (arrow) **(D)**. Bars = 100 μm.

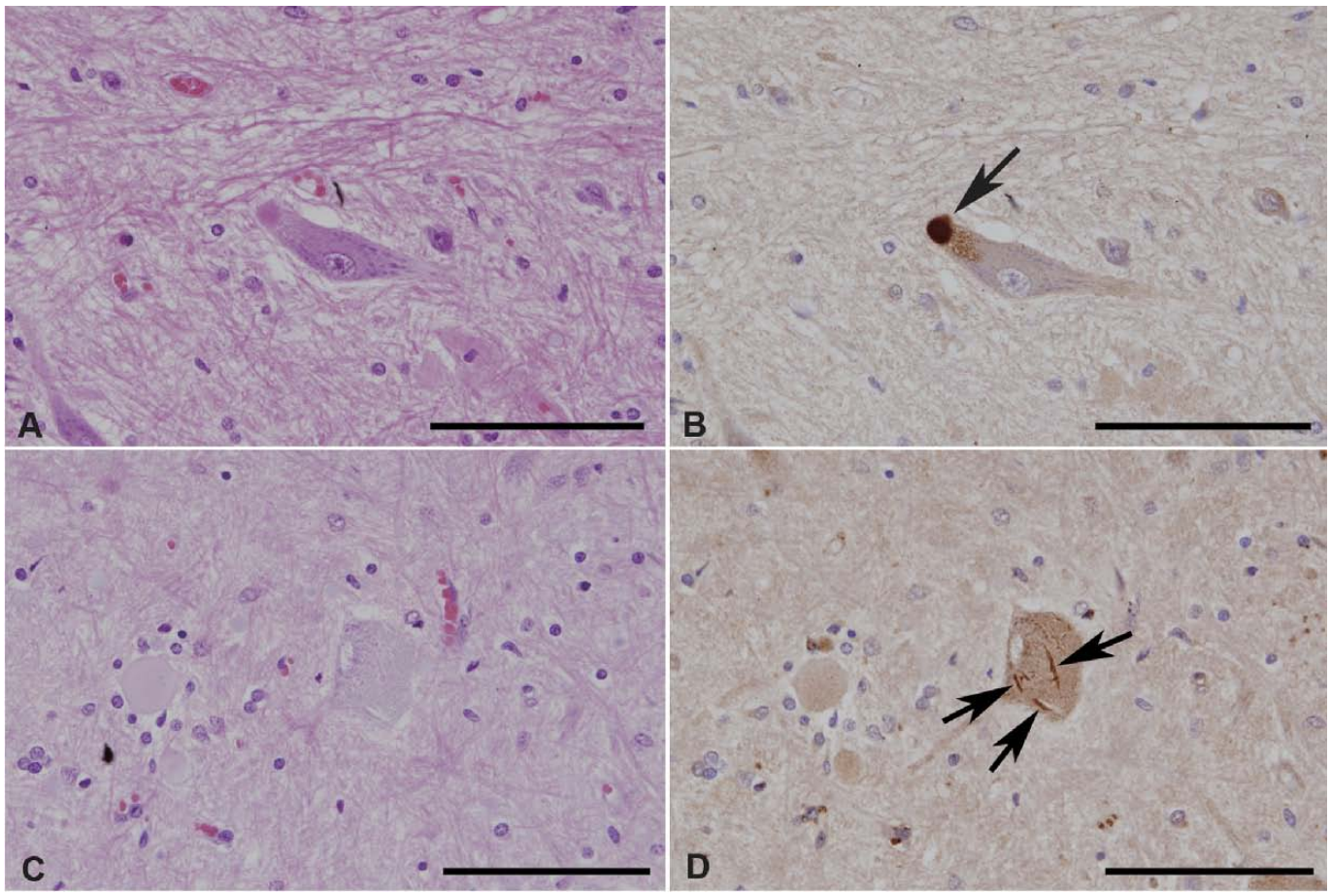

FIGURE 4. Amyotrophic lateral sclerosis patients. **(A, B)** A large anterior horn neuron contains a Lewy body-like hyaline inclusion (**A**, H&E) that is immunostained for p62 (arrow) **(B)**. **(C, D)** A large anterior horn neuron contains skein-like inclusions in the cytoplasm (**C**, H&E) that are immunostained for p62 (**D**, arrows). Bars = 100 μm.

as ''adaptive autophagy,'' is to supply amino acids for cell survival under poor environmental conditions. This type of autophagy is rapidly induced under nutritional deprivation in yeast (25) and in newborn mice (26) and serves as a basic survival strategy in all eukaryotes. The second purpose, known as ''basal autophagy'' or ''constitutive autophagy,'' is to degrade proteins in the cell through continuous operation at a low level irrespective of nutritional stress. Basal autophagy is responsible for the turnover of long-lived proteins, disposal of excess (27) or damaged organelles (28), and clearance of aggregate-prone proteins (29, 30). Thus, under physiological conditions, autophagy has a number of vital roles including the maintenance of the amino acid pool during starvation, prevention of neurodegeneration, antiaging, and tumor suppression (4, 12, 16).

Accumulating evidence indicates that autophagy may protect against the development of a number of neurodegenerative diseases and that a deficiency in autophagy induction could lead to the aggregation of abnormal proteins in neurodegenerative disease models in vitro and in vivo (29–33). Moreover, mice with neural cell–specific knockouts of the autophagy-related 5 (*Atg5*) gene develop progressive motor and behavioral deficits and display abnormal limb-clasping reflexes that are accompanied by the accumulation of cytoplasmic ubiquitin-positive inclusion bodies in neurons (13). These results suggest that the continuous clearance of diffuse cytosolic proteins through basal autophagy is important for preventing the accumulation of abnormal proteins that can disrupt neural function and ultimately lead to neurodegeneration (13). Indeed, the inhibition of mTOR induces autophagy and reduces toxicity of polyglutamine expansion in fly and mouse models of Huntington disease (30). Thus, autophagy may include a protective mechanism to degrade mutant or toxic proteins because defects in autophagy-related pathways contribute to the accumulation of neurotoxic proteins and the ensuing neuronal cell death.

In contrast, autophagy activation may also contribute to neurodegeneration (6, 34). Neonatal mice subjected to hypoxic-ischemic injury show dramatically increased autophagosome formation and extensive hippocampal neuron death, whereas mice deficient in *Atg7*, a gene essential for autophagy induction, show nearly complete protection from both hypoxic-ischemic–induced caspase-3 activation and neuronal death. These data suggest that autophagy plays an

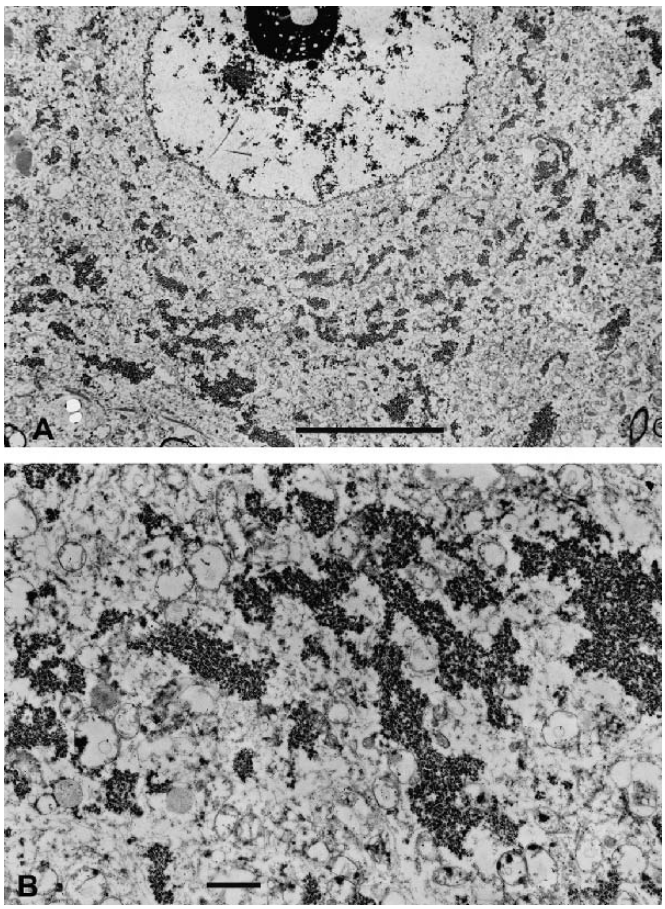

FIGURE 5. Electron microscopy. **(A, B)** A normal-looking motor neuron from a control patient shows no autophagy in the cytoplasm **(A)**. Bar = 10 μm. In a higher magnification, the soma consists of cytoplasmic organelles; there are abundant Nissl bodies and mitochondria **(B)**. Bar = 1 μm.

essential role in triggering neuronal death execution after hypoxic-ischemic injury (35). Targeted disruption of cathepsin D (a major lysosomal protease) in mice results in the aberrant accumulation of autophagosomes that is accompanied by extensive pathologic alterations (36). Moreover, morphologic evidence of autophagy has been reported in neurodegenerative diseases including Parkinson, Huntington, and Alzheimer diseases and in transmissible spongiform encephalopathies (37–40). A recent study using a cellular model of frontotemporal dementia has reported that upregulation of autophagy initiation only led to a greater accumulation of autophagosomes, probably due to the defective autophagic vacuole clearance, thereby increasing stress and subsequent neuronal loss (41). Thus, autophagy is a double-edged sword, and it remains to be elucidated whether autophagy protects against neurodegeneration or has adverse effects on neurons.

LC3, a mammalian homolog of *Atg8*, is processed after posttranslational modifications into the cytosolic form of LC3 (LC3-I), which is then converted to the inner and outer membranes of autophagosomes (LC3-II). Autophagy is induced in axonal dystrophy and degeneration by the association of LC3-I with axonal constituents (42). Thus, LC3 immunopositivity of pericapillary rosettes, which consist of dystrophic axons (24), may be due to the accumulation of autophagy-associated structures and/or the interaction of LC3-I with degenerated axons. The LC3 antibody used in the present study detects both LC3-I and -II. LC3 has been proposed to function as a receptor for a selective substrate, p62 (43), which directly interacts with LC3 and is preferentially degraded by the autophagy-lysosome pathway (43, 44). Because p62 has an ubiquitin-binding domain, ubiquitinated proteins and inclusion bodies may be recruited to the autophagosome membrane via p62 (43, 44); the ubiquitin- and LC3-binding protein p62 may regulate the formation of protein aggregates and is removed by autophagy (33). The main morphologic criterion for recognizing autophagy is identifying cytoplasmic components such as ER and mitochondria within autophagosomes (45). This definition is straightforward and it is usually easy to identify autophagosomes or at least those organelles that envelop cellular contents. Recent

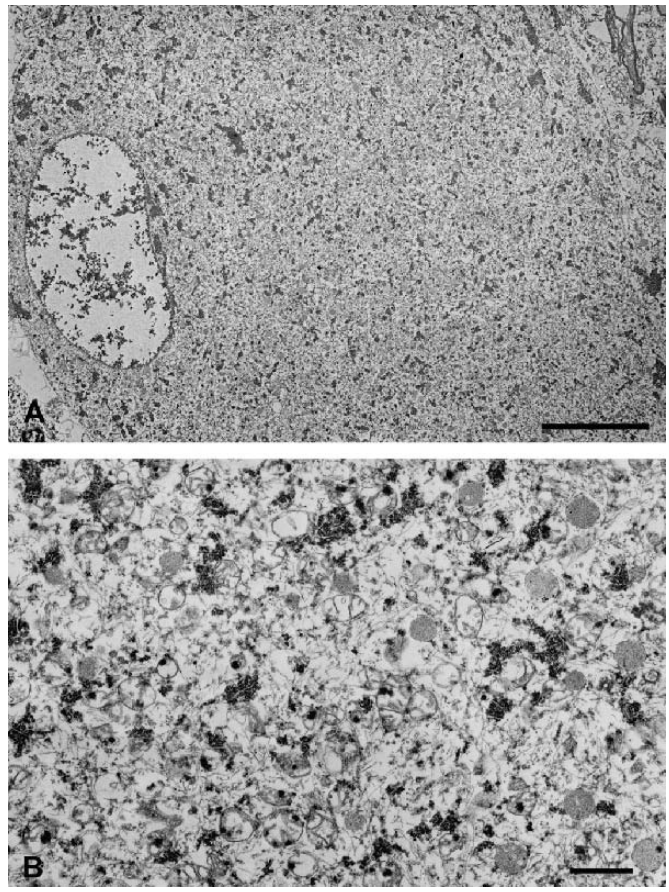

FIGURE 6. Electron microscopy. **(A, B)** A degenerated motor neuron in a control patient shows chromatolytic change with an eccentric nucleus **(A)**. Bar = 10 μm. At a higher magnification, the neuron shows fragmentation and paucity of rough endoplasmic reticulum, abundant mitochondria and lysosomes, but no autophagy-associated morphology **(B)**. Bar = 1 μm.

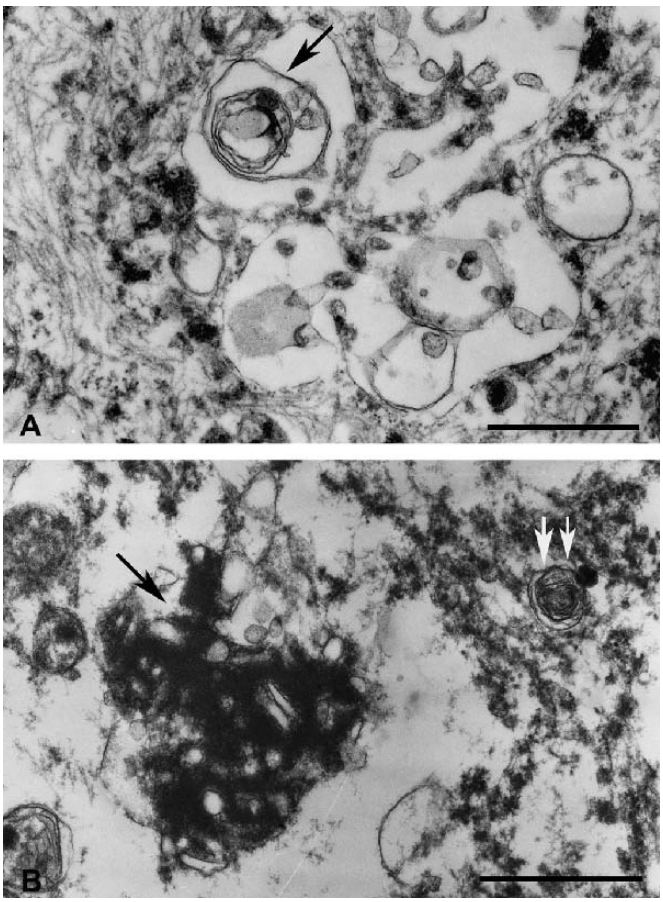

FIGURE 7. Electron microscopy of control patient motor neurons. **(A, B)** A motor neuron with vacuolation in the cytoplasm shows an autophagosome-like structure (arrow) in the perikaryon **(A)**. A degenerated neuron with electron-dense material (single arrow) resembling a Bunina body shows an autolysosome-like structure (double arrows) in the cytoplasm **(B)**. Bars = 1 μm.

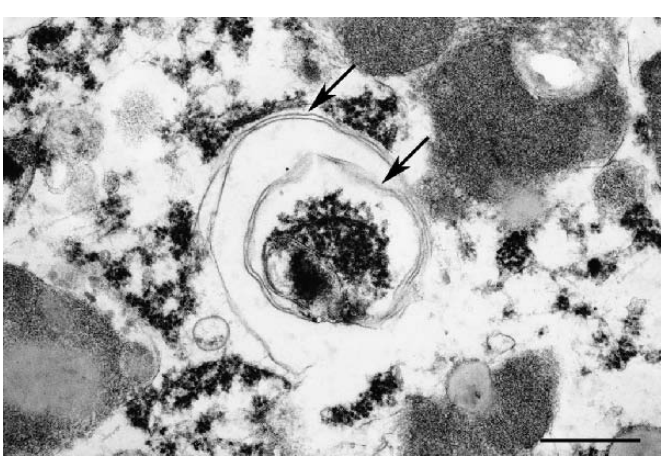

FIGURE 8. An autophagosome surrounded by a double-membrane (arrows) contains mitochondria and ribosome-like structures in the motor neuron of a patient with amyotrophic lateral sclerosis. Bar = 0.5 μm.

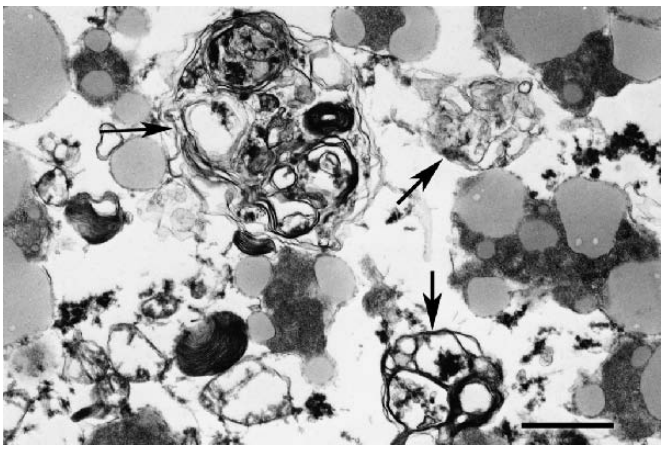

FIGURE 9. Autolysosomes surrounded by a single membrane (arrows) contain cytoplasmic organelles such as mitochondria and multilamellar materials in the motor neuron of a patient with amyotrophic lateral sclerosis. Bar = 1 μm.

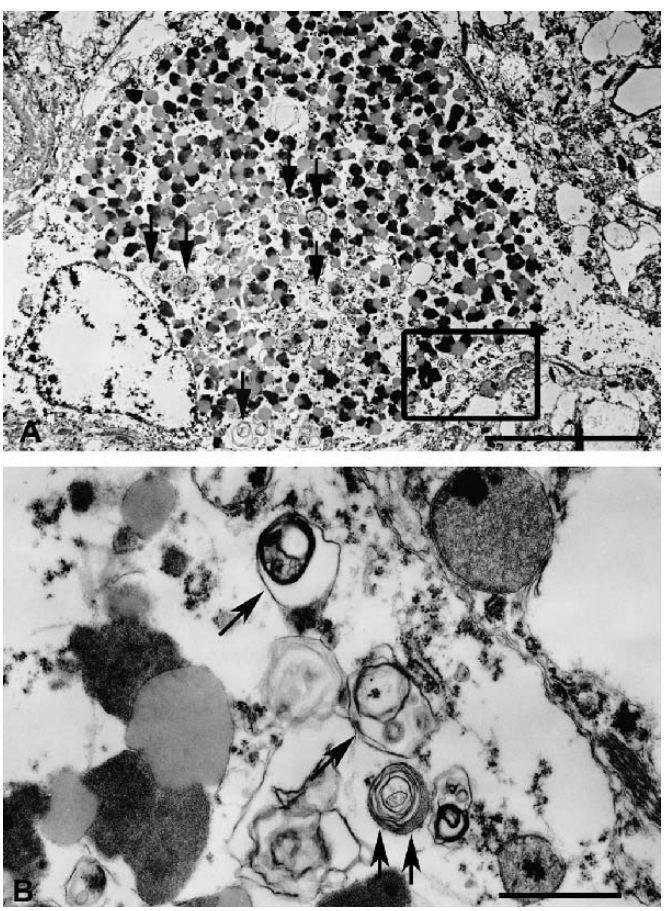

FIGURE 10. Degenerated motor neuron from a patient with amyotrophic lateral sclerosis with pigmentary atrophy. **(A, B)** There are many autophagic features (arrows) in the cytoplasm **(A)**. Bar = 10 μm. In a higher magnification of the portion of **(A)** enclosed within a rectangle there are autophagosomes (single arrow) and an autophagic vacuole-like structure containing a multilamellated structure (double arrows) **(B)**. Bar = 1 μm.

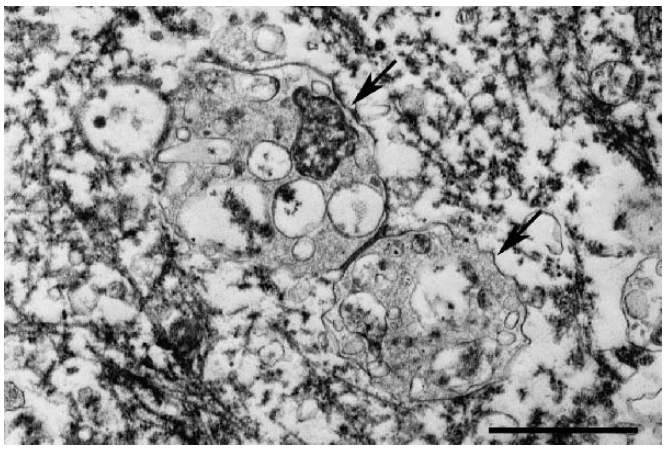

FIGURE 11. Electron microscopy of a round body in a motor neuron from a patient with amyotrophic lateral sclerosis contains autolysosomes (arrows) with mitochondria and vesicles. Bar = 1 μm.

studies have shown that aggregate-prone proteins such as α-synuclein (46), superoxide dismutase (47), and prions (48) are degraded through autophagy.

There have been several reports of autophagy in ALS. Autolysosomal processing of skein-like inclusions is indicated in a single case of ALS (17); autophagy in transgenic mice with G93A mutant *SOD1* gene is increased because of upregulation of LC3-II immunoreactivity (18, 19); and mutations in the autophagy-lysosomal pathway transport machinery have been shown to be associated with frontotemporal dementia and ALS (20). p62 localizes in skein-like inclusions and round bodies, but Bunina bodies are negative for p62 (49). In this study, some normal-appearing as well as some degenerated motor neurons in ALS cases were LC3-immunopositive, ALS-characteristic inclusions were p62-immunopositive, and normal-appearing motor neurons in the controls were not immunostained for either. Moreover, by EM, all ALS patients exhibited autophagosomes and/or autolysosomes in the cytoplasm of both normal-appearing and, more frequently, degenerated motor neurons, and the increase in autophagic processes was closely correlated with ALS-characteristic inclusions. These findings suggest that the primary target of autophagy is not only diffuse cytosolic proteins but also inclusion bodies themselves. In this regard, it is possible that the autophagic pathway could be preferentially activated in the cellular response to misfolded proteins in the ER, because ER stress, defined as the accumulation of misfolded or unfolded proteins in the ER lumen, seems to be involved in the pathomechanism of neurodegeneration of motor neurons in sporadic ALS (50). Moreover, honeycomb-like structures have been observed continuous with the smooth ER in normal cerebella but are more common in a variety of pathologic conditions (51, 52); they have also been reported in the cytoplasm of anterior horn cells in sporadic ALS patients (50, 53). Thus, honeycomb-like structures may be pathologically associated with rER alterations, but it remains to be elucidated further how they relate to ALS.

Activated autophagy suggests expression of involvement in excessive degradation of misfolded proteins or

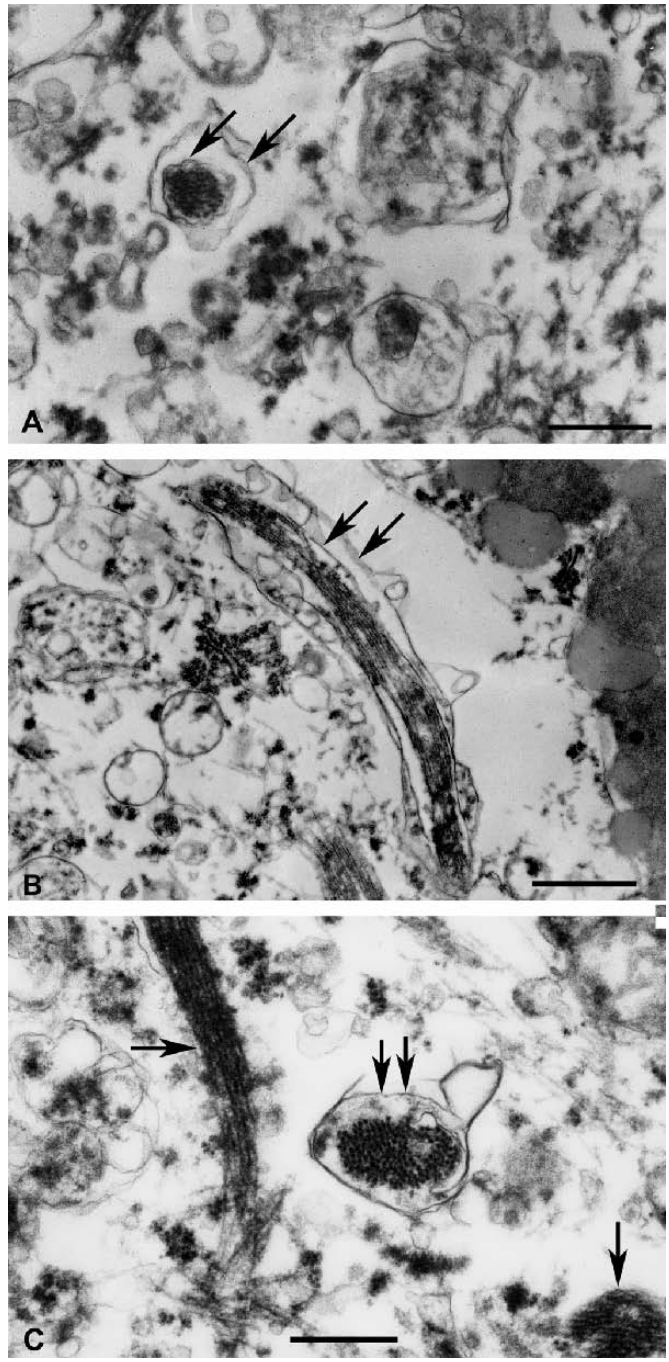

FIGURE 12. Electron microscopy of motor neurons from patients with amyotrophic lateral sclerosis. **(A)** A small skein-like inclusion is engulfed by an autophagosome with a double-membrane (arrows). Bars = 0.5 μm. **(B)** An autophagosome surrounded by a double-membrane (arrows) contains a relatively large skein-like inclusion seen in longitudinal section. Bar = 1 μm. **(C)** An autolysosome surrounded by a single membrane (double arrows) contains a skein-like inclusion in oblique section. There are 2 other skein-like inclusions in the field (arrows). Bar = 0.5 μm.

aggregates, and also suggests that autophagy is a key pathway for the clearance of aggregate-prone cytosolic proteins in ALS. Autophagy upregulation decreases soluble levels of aggregate-prone proteins, decreases the proportion of cells with inclusions, and attenuates toxicity (28, 54, 55). In contrast, excessive autophagy seems capable of promoting cell injury (56). In this study, the absence of autophagosomes in the cytoplasm of normal-looking motor neurons in controls is consistent with previous reports that the levels of autophagosomes detected in neurons are very low under normal and even starvation conditions (22). By contrast, both autophagosomes and autolysosomes were far more abundant in the cytoplasm of motor neurons in patients with sporadic ALS, which is consistent with typical results of the induction of autophagy (57). Thus, the difference in the frequency of appearance of autophagic processes between the controls and sporadic ALS is considerable. These findings suggest that in sporadic ALS mild to moderate upregulation of autophagic activity at the early stage of motor neuron degeneration might play a protective role in the segregation of abnormal proteins by rapidly forming aggregates or inclusion bodies via p62 to avoid cellular dysfunction; at the later stages, autophagy insufficiency or deficiency caused by overproduction of misfolded proteins or aggregates may contribute to the neurodegeneration of motor neurons, eventually leading to autophagic cell death.

Some reports suggest that autophagosomes can be generated locally within the axon and then transported in a retrograde direction along the axon toward the cell body for fusion with lysosomes (58, 59). The fusion of the autophagosome with the lysosome is controlled by the dynein/dynactin complex, which is associated with retrograde axonal transport (60). When a mutation of either dynein or dynactin occurs, there is impairment of the fusion and the autophagolysosome is not produced (60). Activated autophagy in the cytoplasm of motor neurons combined with no activation of autophagy in the axons observed in this study suggests that the autophagosome and autolysosome accumulation in the somata of motor neurons is not due to the upregulation of autophagy within the axon but due to the activation of autophagy in the cytoplasm in patients with sporadic ALS.

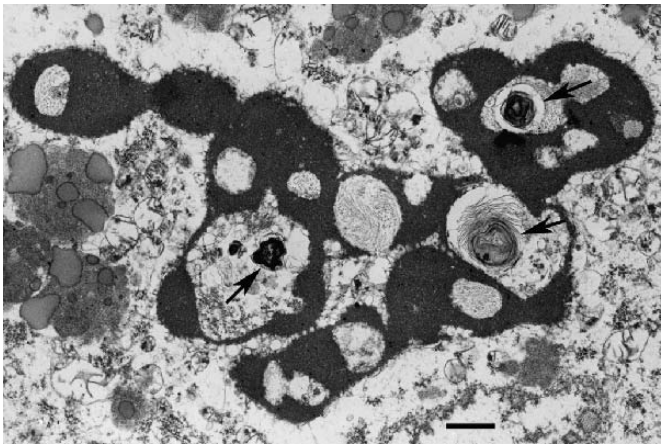

FIGURE 13. A Bunina body contains autophagic multilamellar bodies (arrows) in a patient with amyotrophic lateral sclerosis. Bar = 1 μm.

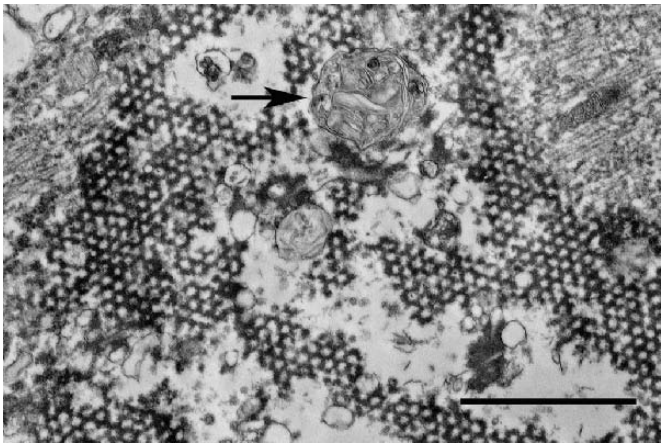

FIGURE 14. An autolysosome (arrow) within a honeycomb-like structure. Bar = 1 μm.

ACKNOWLEDGMENTS

The author thanks Dr. M. Kobayashi and Ms. N. Sakayori for their technical help with the immunohistochemical study.

REFERENCES

1. Goldberg AL. Protein degradation and protection against misfolded or damaged proteins. Nature 2003;426:895–99
2. Klionsky DJ. Emr SD. Autophagy as a regulated pathway of cellular degradation. Science 2000;290:1717–21
3. Mizushima N, Ohsumi Y, Yoshimori T. Autophagosome formation in mammalian cells. Cell Struct Funct 2002;27:421–29
4. Levine B, Kroemer G. Autophagy in the pathogenesis of disease. Cell 2008;132:27–42
5. Baehrecke EH. Autophagy: Dual roles in life and death? Nat Rev Mol Cell Biol 2005;6:505–10
6. Shintani T, Klionsky DJ. Autophagy in health and disease: A double-edged sword. Science 2004;306:990–95
7. Borsello T, Croquelois K, Hornung JP, et al. *N*-methyl-D-aspartate–triggered neuronal death in organotypic hippocampal cultures is endocytic, autophagic and mediated by the c-Jun N-terminal kinase pathway. Eur J Neurosci 2003;18:473–85
8. Levine B, Klionsky DJ. Development by self-digestion: Molecular mechanisms and biological functions of autophagy. Dev Cell 2004;6:463–77
9. Cuervo AM, Bergamini E, Brunk UT, et al. Autophagy and aging: The importance of maintaining "clean" cells. Autophagy 2005;1:131–40
10. Kondo Y, Kanazawa T, Sawaya R, et al. The role of autophagy in cancer development and response to therapy. Nat Rev Cancer 2005;5:726–34
11. Chu CT. Autophagic stress in neuronal injury and disease. J Neuropathol Exp Neurol 2006;65:423–32
12. Mizushima N, Levine B, Cuervo AM, et al. Autophagy fights disease through cellular self-digestion. Nature 2008;451:1069–75
13. Hara T, Nakamura K, Matsui M, et al. Suppression of basal autophagy in neural cells causes neurodegenerative disease in mice. Nature 2006;441:885–89
14. Komatsu M, Waguri S, Chiba T, et al. Loss of autophagy in the central nervous system causes neurodegeneration in mice. Nature 2006;441:880–84
15. Nixon RA. Autophagy in neurodegenerative disease: Friend, foe or turncoat? Trends Neurosci 2006;29:528–35
16. Rubinsztein DC. The roles of intracellular protein-degradation pathways in neurodegeneration. Nature 2006;443:780–86
17. Nakano I, Shibata T, Uesaka Y. On the possibility of autolysosomal

processing of skein-like inclusions. Electron microscopic observation in a case of amyotrophic lateral sclerosis. J Neurol Sci 1993;120:54–59
18. Morimoto N, Nagai M, Ohta Y, et al. Increased autophagy in transgenic mice with a G93A mutant *SOD1* gene. Brain Res 2007;1167:112–17
19. Li L, Zhang X, Le W. Altered macroautophagy in the spinal cord of SOD1 mutant mice. Autophagy 2008;4:290–93
20. Rusten TE, Simonsen A. ESCRT functions in autophagy and associated disease. Cell Cycle 2008;7:1166–72
21. Kabeya Y, Mizushima N, Ueno T, et al. LC3, a mammalian homologue of yeast *Apg8p*, is localized in autophagosome membrane after processing. EMBO J 2000;19:5720–28
22. Mizushima N, Yamamoto A, Matsui M, et al. In vivo analysis of autophagy in response to nutrient starvation using transgenic mice expressing a fluorescent autophagosome marker. Mol Biol Cell 2004;15: 1101–11
23. Ichimura Y, Kumamomidou T, Sou YS, et al. Structural basis for sorting mechanism of p62 in selective autophagy. J Biol Chem 2008;283: 22847–57
24. Sasaki S, Iwata M. Immunocytochemical and ultrastructural study of pericapillary rosettes in amyotrophic lateral sclerosis. Acta Neuropathol 1997;94:338–44
25. Tsukada M, Ohsumi Y. Isolation and characterization of autophagy-defective mutants of *Saccharomyces cerevisiae*. FEBS Lett 1993;333: 169–74
26. Kuma A, Hatano M, Matsui M, et al. The role of autophagy during the early neonatal starvation period. Nature 2004;432:1032–36
27. Iwata J, Ezaki J, Komatsu M, et al. Excess peroxisomes are degraded by autophagic machinery in mammals. J Biol Chem 2006;281:4035–41
28. Elmore SP, Qian T, Grissom SF, et al. The mitochondrial permeability transition initiates autophagy in rat hepatocytes. FASEB J 2001;15: 2286–87
29. Fortun J, Dunn WA Jr, Joy S, et al. Emerging role for autophagy in the removal of aggresomes in Schwann cells. J Neurosci 2003;23:10672–80
30. Ravikumar B, Vacher C, Berger Z, et al. Inhibition of mTOR induces autophagy and reduces toxicity of polyglutamine expansion in fly and mouse models of Huntington disease. Nat Genet 2004;36:585–95
31. Ravikumar B, Duden R, Rubinsztein DC. Aggregate-prone proteins with polyglutamine and polyalanine expansions are degraded by autophagy. Hum Mol Genet 2002;11:1107–17
32. Iwata A, Christianson JC, Bucci M, et al. Increased susceptibility of cytoplasmic over nuclear polyglutamine aggregates to autophagic degradation. Proc Natl Acad Sci U S A 2005;102:13135–40
33. Komatsu M, Waguri S, Koike M, et al. Homeostatic levels of p62 control cytoplasmic inclusion body formation in autophagy-deficient mice. Cell 2007;131:1149–63
34. Yue Z, Horton A, Bravin M, et al. A novel protein complex linking the δ_2 glutamate receptor and autophagy: Implications for neurodegeneration in lurcher mice. Neuron 2002;35:921–33
35. Koike M, Tadakoshi M, Gotoh K, et al. Inhibition of autophagy prevents hippocampal pyramidal neuron death after hypoxic-ischemic injury. Neurobiology 2008;172:454–69
36. Kohli L, Roth KA. Autophagy. Cerebral home cooking. Am J Pathol 2010;176:1065–71
37. Qin ZH, Wang Y, Kegel KB, et al. Autophagy regulates the processing of amino terminal huntingtin fragments. Hum Mol Genet 2003;12:3231–44
38. Anglade P, Vyas S, Javoy-Agid F, et al. Apoptosis and autophagy in nigral neurons of patients with Parkinson's disease. Histol Histopathol 1997;12:25–31
39. Nixon RA, Wegiel J, Kumar A, et al. Extensive involvement of autophagy in Alzheimer disease: An immuno-electron microscopy study. J Neuropathol Exp Neurol 2005;64:113–22
40. Liberski PP, Sikorska B, Bratosiewicz-Wasik J, et al. Neuronal cell death in transmissible spongiform encephalopathies (prion diseases) revisited: From apoptosis to autophagy. Int J Biochem Cell Biol 2004;36:2473–90
41. Lee JA, Gao FB. Inhibition of autophagy induction delays neuronal cell loss caused by dysfunctional ESCRT-III in frontotemporal dementia. J Neurosci 2009;29:8506–11
42. Wang QJ, Ding Y, Kohtz DS, et al. Induction of autophagy in axonal dystrophy and degeneration. J Neurosci 2006;26:8057–68
43. Bjørkøy G, Lamark T, Brech A, et al. p62/SQSTM1 forms protein aggregates degraded by autophagy and has a protective effect on huntingtin-induced cell death. J Cell Biol 2005;171:603–14
44. Pankiv S, Clausen TH, Lamark T, et al. p62/SQSTM1 binds directly Atg8/LC3 to facilitate degradation of ubiquitinated protein aggregates by autophagy. J Biol Chem 2007;282:24131–45
45. De Duve C, Wattiaux R. Functions of lysosomes. Annu Rev Physiol 1966;28:435–92
46. Webb JI, Ravikumar B, Atkins J, et al. α-Synuclein is degraded by both autophagy and the proteasome. J Biol Chem 2003;278:25009–13
47. Fornai F, Longone P, Cafaro L, et al. Lithium delays progression of amyotrophic lateral sclerosis. Proc Natl Acad Sci U S A 2008;105: 2052–57
48. Aguib Y, Heiseke A, Gilch S, et al. Autophagy induction by trehalose counteracts cellular prion infection. Autophagy 2009;5:361–69
49. Mizuno Y, Amari M, Takatama M, et al. Immunoreactivities of p62, an ubiquitin-binding protein, in the spinal anterior horn cells of patients with amyotrophic lateral sclerosis. J Neurol Sci 2006;249:13–18
50. Sasaki S. Endoplasmic reticulum stress in motor neurons of spinal cord in patients with sporadic ALS. J Neuropathol Exp Neurol 2010;69:346–55
51. Hirano A, Sax DS, Zimmermann HM. The fine structure of the cerebella of jimpy mice and their ''normal'' litter mates. J Neuropathol Exp Neurol 1969;28:388–400
52. Sotelo C, Palay SL. Altered axons and axon terminals in the lateral vestibular nucleus of the rat: Possible example of axonal remodeling. Lab Invest 1971;25:653–71
53. Sasaki S, Hirano A, Donnenfeld H, et al. Honeycomb-like and aggregated filamentous structures in the anterior horn cells. Electron microscopic study in cases of amyotrophic lateral sclerosis. Shinkeinaika (Tokyo) 1983;18:298–301
54. Sarkar S, Floto RA, Berger Z, et al. Lithium induces autophagy by inhibiting inositol monophosphatase. J Cell Biol 2005;170:1101–11
55. Williams A, Sarkar S, Cuddon P, et al. Novel targets for Huntington's disease in an mTOR-independent autophagy pathway. Nat Chem Biol 2008;4:295–305
56. Levine B, Yuan J. Autophagy in cell death: An innocent convict? J Clin Invest 2005;115:2679–88
57. Mizushima N. Methods in mammalian autophagy research. Cell 2010; 140:313–26
58. Hollenbeck PJ. Products of endocytosis and autophagy are retrieved from axons by regulated retrograde organelle transport. J Cell Biol 1993;121: 305–15
59. Yue Z. Regulation of neuronal autophagy in axon: Implication of autophagy in axonal function and dysfunction/degeneration. Autophagy 2007;3:139–41
60. Pasquali L, Longone P, Isidoro C, et al. Autophagy, lithium, and amyotrophic lateral sclerosis. Muscle Nerve 2009;40:173–94

